Scanning Microscopy

Volume 7 | Number 4 Article 18

12-26-1993

Scanning Electron Microscopy of High-Pressure-Frozen Sea Urchin Embryos

Paul Walther
University of Wisconsin-Madison

Ya Chen
University of Wisconsin-Madison

Marek Malecki
University of Wisconsin-Madison

Sara L. Steffen Zoran
University of Wisconsin-Madison

Gerald P. Schatten
University of Wisconsin-Madison

See next page for additional authors

Scanning Electron Microscopy of High-Pressure-Frozen Sea Urchin Embryos

Authors

Paul Walther, Ya Chen, Marek Malecki, Sara L. Steffen Zoran, Gerald P. Schatten, and James B. Pawley

Scanning Microscopy, Vol. 7, No. 4, 1993 (Pages 1283-1293)
Scanning Microscopy International, Chicago (AMF O'Hare), IL 60666 USA

0891-7035/93$5.00+.00

SCANNING ELECTRON MICROSCOPY OF HIGH-PRESSURE-FROZEN SEA URCHIN EMBRYOS

Paul Walther[1,*], Ya Chen[1], Marek Malecki[1], Sara L. Steffen Zoran[2], Gerald P. Schatten[2], James B. Pawley[2]

[1]Integrated Microscopy Resource for Biomedical Research, University of Wisconsin-Madison
1675 Observatory Drive, Madison, WI, 53706

[2]Zoology Department, University of Wisconsin-Madison, 1117 W. Johnson St., Madison, WI, 53706

(Received for publication August 2, 1993, and in revised form December 26, 1993)

Abstract

High-pressure-freezing permits direct cryo-fixation of sea urchin embryos having a defined developmental state without the formation of large ice crystals. We have investigated preparation protocols for observing high-pressure-frozen and freeze-fractured samples in the scanning electron microscope. High-pressure-freezing was superior to other freezing protocols, because the whole bulk sample was reasonably well frozen and the overall three-dimensional shape of the embryos was well preserved. The samples were either dehydrated by freeze-substitution and critical-point-drying, or imaged in the partially hydrated state, using a cold stage in the SEM. During freeze-substitution the samples were stabilized by fixatives. The disadvantage of this method was that shrinking and extraction effects, caused by the removal of the water, could not be avoided. These disadvantages were avoided when the sample was imaged in the frozen-hydrated state using a cold-stage in the SEM. This would be the method of choice for morphometric studies. Frozen-hydrated samples, however, were very beam sensitive and many structures remained covered by the ice and were not visible. Frozen-hydrated samples were partially freeze-dried to make visible additional structures that had been covered by ice. However, this method also caused drying artifacts when too much water was removed.

Key Words: Scanning electron microscopy (SEM), low temperature SEM, high pressure freezing, embryos, sea urchin, cryo-SEM, freeze-substitution, double layer coating, low voltage SEM.

*Address for correspondence and **present address**:
Paul Walther,
Laboratory of Electron Microscopy 1,
Department of Cell Biology,
ETH Zurich,
Schmelzbergstrasse 7,
CH-8092 Zurich, Switzerland
Telephone Number: +41 1 632 39 37
FAX Number: +41 1 261 03 91

Introduction

Rapid freezing is the best initial fixation step to immobilize a biological sample under defined physiological conditions (reviewed by Sitte et al. 1987). Cryo-fixation is much faster than chemical fixation: it stops all physiological processes within a few milliseconds. In contrast to chemical fixation, which immobilizes only structural proteins and some lipids, all components including diffusible proteins and ions are maintained in the frozen sample (reviewed by Zierold, 1991). The main problem related to cryo-fixation is distortion of the biological structure by the formation of ice crystals that occurs if cooling rates are insufficient. Because the thermal conductivity of frozen water is relatively poor, a cooling rate high enough to prevent the formation of large ice crystals (at ambient pressure) is only obtained in the outermost layer of a specimen (up to a depth of about 10 μm from the surface). Thicker specimens, however, can be cryo-fixed by high-pressure-freezing (Moor and Riehle, 1968) where the specimen is frozen while applying simultaneously a pressure of 2000 bar. This pressure suppresses the formation of ice crystals (reviewed by Moor, 1987). In practical work, the method allows for cryo-fixation of fresh cell and tissue samples up to a thickness of about 200 μm without visible ice crystal segregation patterns.

High resolution scanning electron microscopy (SEM) is a very suitable technique to image high-pressure-frozen samples because this technique: 1.) works not only at high magnifications but permits overviews of large areas at magnifications down to 100 x. This advantage permits one to determine the orientation of complex tissue samples; 2.) allows for the observation of bulk samples, that do not need to be thin-sectioned or replicated; 3.) can be used with a cold-stage, that permits high-pressure-frozen specimens to be directly analyzed in the hydrated state (Echlin, 1971).

The SEM images the sample surface. To see the intracellular biological structures, a frozen sample must be freeze-fractured and/or the surface ice must be removed. This can be achieved either by sublimation (usually referred to as freeze-drying or freeze-etching) or by freeze-substitution, where the ice is substituted at cold temperatures by an organic solvent, which is then usually removed by critical-point-drying (Barlow and Sleigh, 1979). However, every method of water removal bears the danger of drying artefacts. In this paper we study the potential and limitations of freeze-substitution, critical-point-drying and freeze-drying for the SEM-observation of high-pressure-frozen and cryo-fractured samples.

Sea urchin eggs and embryos were used as model systems in which to perfect and evaluate ultrastructural methods. The 80 μm cells provided a rigorous system to explore the depth of proper specimen preservation after high-pressure-freezing. Furthermore, eggs and embryos displayed all the dynamics of other cells including alterations in membrane behaviour, cytoskeletal activity and chromatin changes throughout the cell cycle.

Materials and Methods

Sea urchin egg and embryo preparation

Lytechinus pictus or *Strongylocentrotus purpuratus* sea urchin gametes were collected by inducing the urchin to spawn by a 0.55 M KCl intracoelomic injection. Eggs were released into artificial sea water and sperm were collected dry on ice. Eggs were dejellied by passing them through a 74 µm Nitex mesh 4-5 times followed by rinsing. After monospermic fertilization, some eggs were stripped of their fertilization coats by a 10-15 min treatment with 6 mM Dithiothreitol and 0.01 % trypsin in artificial sea water and cultured in artificial sea water until the desired stage was obtained.

High-pressure-freezing

A commercial high-pressure-freezer (HPM 010; Bal-Tec) was used (Moor, 1987). Gold planchets (diameter 3 mm, central cavity about 0.3 mm; Bal-Tec) were filled with a solution of 15 % gelatine in artificial sea water to improve the mechanical contact between specimen and specimen holder. The sea urchin embryos were added as soon as the gelatine was nearly solid. A droplet of the suspension with sea urchin eggs, or sea urchin embryos either 1 h or 24 h after fertilization was added into the planchettes. A second planchette was put on the top and all cavities in between the two planchets were filled with hexadecene. (Hexadecene is not miscible with water and therefore does not act as a cryo-protectant; Its purpose is to exclude any gas bubbles that would collapse when subjected to the high pressure liquid nitrogen; Studer et al., 1989. Hexadecene may cause allergic reactions, Tobler and Freiburghaus, 1991; therefore, skin contact was avoided.) The holder was then mounted in the freezing chamber of the HPM 010 and frozen with superbaric liquid nitrogen at a pressure of about 2000 bar. The frozen samples were then stored in liquid nitrogen.

Freeze-substitution and critical-point-drying

The preparation protocol for freeze-substitution and critical-point-drying is outlined in Figure 1. The frozen samples were cryo-fractured in liquid nitrogen with a scalpel. Afterwards, freeze-substitution was carried out as described by Müller et al. (1980): The freeze-substitution medium consisted of methanol containing 0.5 % osmium tetroxide, 3 % glutaraldehyde and 3 % water. The samples were freeze-substituted in a Bal-Tec FSU 010 for 8 h at 183 K, 8h at 213 K and 5 h at 243 K and 1 h at 273 K. After washing with cold methanol (273 K), the samples were warmed up to room temperature, washed with ethanol and critical-point-dried (Anderson, 1951; Barlow and Sleigh, 1979) as described by Ris (1985) using carbon dioxide.

The dried samples were double-layer-coated for imaging with backscattered electrons (BSE; Walther and Hentschel, 1989). First, a thin layer of platinum was applied by ion beam sputter coating (Franks et al., 1980) in an Ion Tech apparatus (distributed by VCR). The average thickness estimate of 3 nm of platinum is based on comparative BSE images (Walther et al., 1991). The coating conditions were: Argon pressure in the specimen chamber: 4 x 10^{-5} mbar; time: 6 min; Ar^+ beam current: 4 mA at 10 kV. The specimen was rotated and tumbled during coating. After platinum coating, specimens were coated with an additional layer of carbon with a thickness of 5 to 10 nm by indirect evaporation. These samples (Fig. 5 to Fig. 13) were then imaged in a Hitachi S-900 SEM at ambient temperature with backscattered electrons.

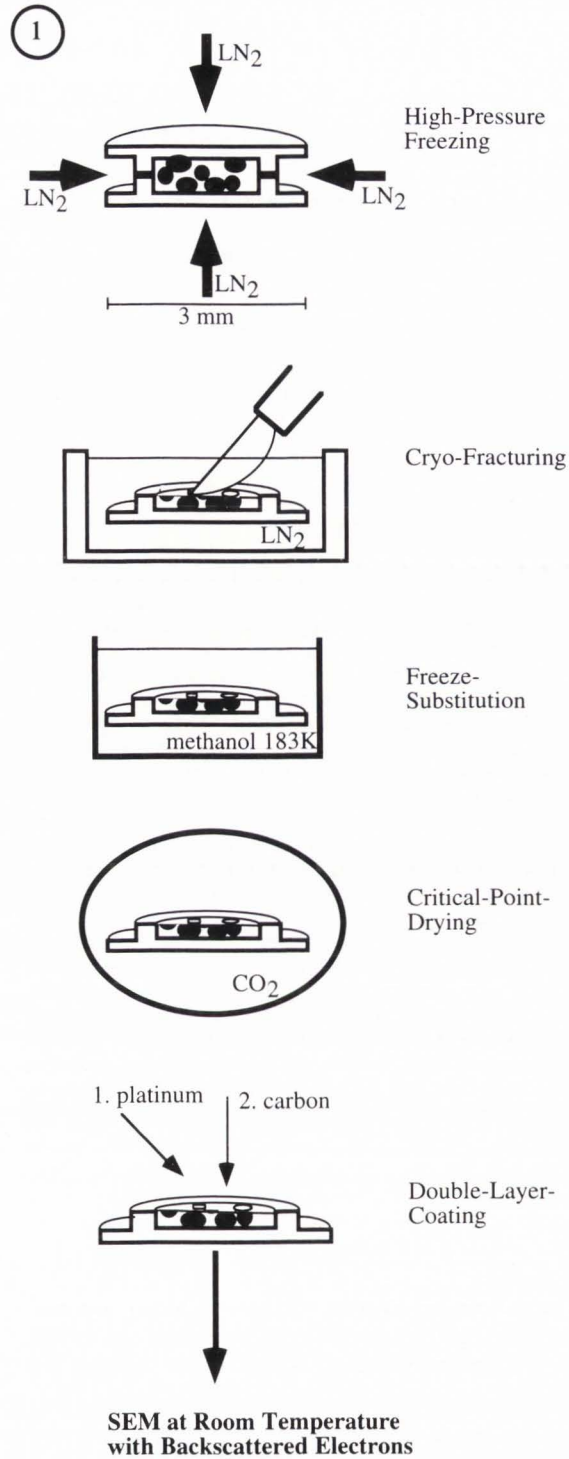

Figure 1. Diagram of the preparation procedure of the freeze-substituted and critical-point-dried samples (Fig. 3 to Fig.13).

Partial freeze-drying, cryo-coating and cryo-transfer

The preparation diagram for partially freeze-dried samples is outlined in Fig. 2. They were cryo-fractured in liquid nitrogen with a scalpel and then coated in a MED 010 planar magnetron sputtering device (Bal-Tec) modified to allow for coating of frozen-hydrated or partially freeze-dried samples. This device is equipped with a cold finger and an insertion adapter for the Gatan cryo-stage (HR 010, Bal-Tec; developed by Hermann and Müller, 1991) and this permits sputter coating of cold samples that are mounted on the cold-stage. The unit is evacuated with a turbo molecular pump backed by a rotary pump.

The fractured samples, mounted on the Gatan stage were transferred into the cryo-coating unit with the sample cooled. The sample was protected from contamination by moisture in the air by means of a shutter on the stage and a small amount of evaporating liquid nitrogen trapped between the shutter and the specimen. The transfer from liquid nitrogen into the specimen preparation chamber took about five seconds until the pumps were started. After about 10 min, a vacuum of 5×10^{-6} mbar was reached. The fully hydrated samples (Fig. 14) were coated immediately after opening the shutter at 148 K for 15 s. The samples in Fig. 15 were partially dehydrated ("etched") by opening the shutter at about 183 K for 15 min, and those for Figs. 16 and 17 at about 163 K for 5 min. Then the shutter was closed until conditions were adjusted to start sputtering. Platinum was used as a sputter target. The sputter conditions were: argon gas pressure 2×10^{-2} mbar; discharge current 25 mA. After reaching constant sputtering conditions, the shutter was opened and the specimen was coated for 30 sec. After coating, the shutter was closed. The chamber was flooded with argon gas and the Gatan cryo-stage, with its attached sample, was removed and transferred in cold nitrogen gas into the SEM. We did not directly measure the coat thickness, however, by comparisons with previously published data (Walther et al., 1990) it is estimated to be below 3 nm (average).

Scanning electron microscopy

A Hitachi S-900, in-lens, field emission SEM (Nagatani et al., 1987) with modifications to enhance the performance of the microscope at low primary acceleration voltages (V_O; Pawley, 1990; Pawley and Erlandsen, 1989) was used. To minimize hydrocarbon residues in the vacuum, all rough pumping was performed by oil-free molecular drag pumps (Danielson, 1987). The microscope is equipped with a highly sensitive annular YAG-detector for backscattered electrons (Autrata et al., 1992).

The freeze-substituted and critical-point-dried samples that had been double-layer-coated (Fig. 3 to Fig. 13) were imaged with the backscattered electron signal (except for Fig. 12 which is a secondary electron image) at ambient temperature. The accelerating voltage of the primary beam (V_O) was 4 kV. These conditions were found to be optimal for imaging the platinum layer of a double-layer-coated sample (Walther et al., 1991). Stereo pairs were obtained by tilting the sample + and - 4°. The stereo pairs can be viewed with regular stereo magnifier viewers. They are mounted so that the central parts of the images overlap and are perceived in stereo. The peripheral areas do not overlap which is consistent with our natural viewing.

The partially freeze-dried samples (Figs. 14 to 17) were observed while mounted on the Gatan cryo-stage using the secondary electron signal. During transfer and observation the temperature never rose above 138 K. The cryo-stage was inserted into the microscope and the specimen chamber was pumped with a turbo molecular pump for about 10 min to reduce partial pressure of water vapour in the specimen chamber, before opening the shutter. Specimens were observed at 138 K; V_O was 3 kV.

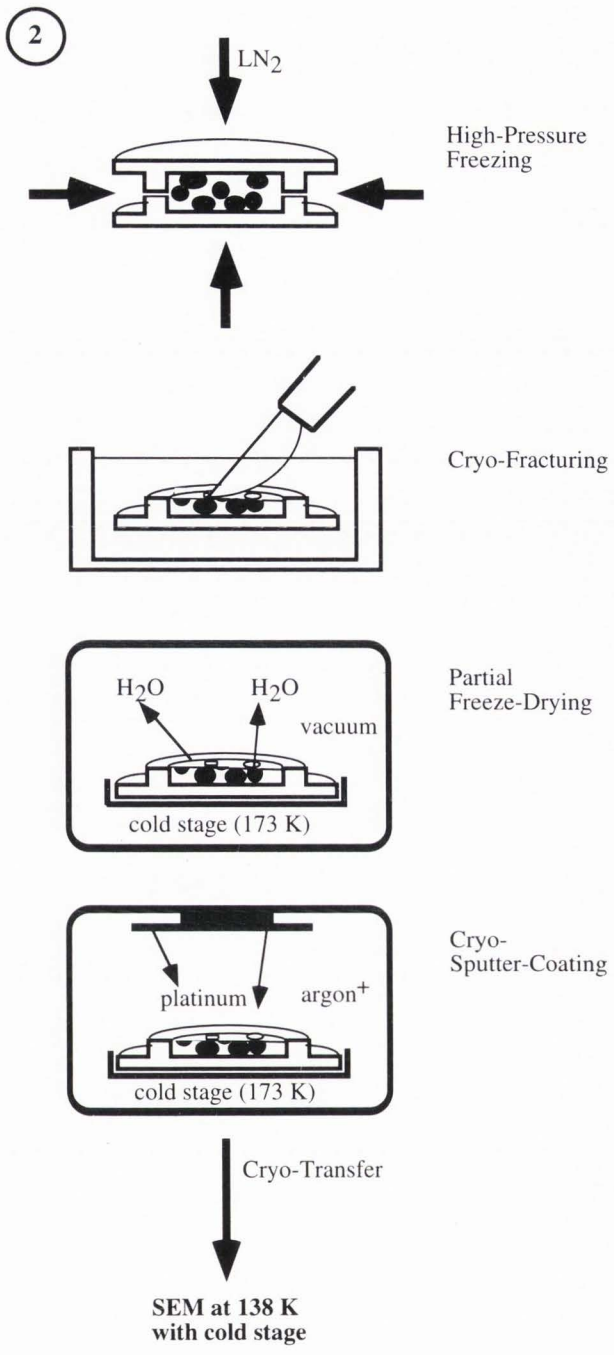

Figure 2. Diagram of the preparation procedure of the partially freeze-dried samples (Fig. 14 to 17)

Sample preparation for transmission electron microscopy (TEM)

For TEM observation (Fig. 3 and 4) the high-pressure-frozen samples were freeze-substituted and embedded as described by Müller et al. (1980) and by Studer et al. (1989)

using 2% osmium tetroxide in acetone as the substitution medium. Samples were embedded in Epon (Luft, 1961), ultra-thin sectioned and post-stained with uranyl acetate and lead citrate (5 min each; Reynolds, 1963). The samples were imaged in a JEOL 100S TEM at an accelerating voltage of 80 kV.

Results

Freeze-substitution and embedding for TEM

To investigate whether the samples are frozen without major ice crystal artefacts, high-pressure-frozen sea urchin embryos were imaged in the TEM as described in material and methods. Figure 3 shows a portion of a cell with the nucleus on the left and the cytoplasm with yolk granules on the right. Fig. 4 shows a Golgi with vesicles and a centriole (c). Large areas of the high-pressure-frozen TEM-samples show good preservation of ultrastructural features and no indication of ice crystal segregation patterns.

Freeze-substitution and critical-point-drying for the SEM

Fig. 5 to Fig. 13 are the samples that were high-pressure-frozen, cryo-fractured, freeze-substituted, critical-point-dried and coated as outlined in Fig. 1. Images were obtained using the backscattered electron signal. Fig. 5 shows a low magnification overview of several fractured sea urchin embryos (first mitotic division, about 2 h after fertilization, black arrow depicts a hyaline layer). Large areas of fracture faces are obtained by this method. Fig. 6 is a high magnification image (100,000 x) of the same specimen showing a fractured vesicle. These two figures demonstrate the wide range of magnification that can be achieved with the high resolution SEM.

Figs. 7 to 11 represent stereo pairs of sea urchin embryos at different developing stages. Fig. 7 is a cell undergoing the first mitotic division. The distribution of yolk granules is uneven, they are absent in the middle of the cytoplasm, the area of the chromosomes and the mitotic spindle. The embryo surface is covered by microvilli and by the fertilization envelope which is formed after fertilization.

Fig. 8 is a mesenchyme blastula stage sea urchin embryo. Some primary mesenchymal cells are visible in the blastocoel. The stereo image shows the good three-dimensional preservation of the embryo.

Figs. 9, 10, and 11 represent different magnifications of the same gastrula stage embryo. Also in this sample three dimensional aspects are preserved. The fractured cells are filled with yolk granules. Some of the yolk granules are cracked (Fig. 11).

Fig. 12 is the surface of an unfertilized egg. It is covered with short microvilli and a fine structure that possibly represents the carbohydrate residues of glycoproteins.

Fig. 13 shows a fertilized egg at the upper left hand side and an unfertilized egg at the lower right hand side. The elongated microvilli appear only at the surface of the fertilized egg.

Partial freeze-drying for the cryo-SEM

Figs. 14 to 17 demonstrate the effects of partial freeze-drying (etching). (The samples are prepared as outlined in Fig. 2.) Because of the cold temperatures and the absence of etching (Fig. 14), all the cavities in between the biological structures are still filled with ice. The biological information obtained is very similar to the information in a freeze-fracture replica in TEM. These samples are very sensitive to beam induced mass loss, but essentially free of shrinking and collapse. At long etching times and relatively warm temperatures (183 K, 15 min) the ice sublimes and additional structures become visible (Fig. 15) but membrane structures generally collapse. Membranes are better preserved if less water is removed by etching at a lower temperature (163 K; Figs. 16 and 17).

Discussion

Freezing

High-pressure-freezing is a very suitable technique for cryo-fixing sea urchin embryos. The embryos fit well into the small planchets and, therefore, can be frozen without any pretreatment such as sectioning, chemical fixation or cryo-protection. Using high-pressure-freezing, the whole 80 µm embryo is reasonably well frozen, in contrast to other freezing techniques where only a small (2 to 10 µm) strip at the specimen surface can be frozen without major ice crystal damage (reviewed by Sitte et al., 1987). In addition, the stereo pairs (Fig. 7 to Fig. 11) reveal good preservation of the spherical structure of the embryo. We could not identify any artifact produced by the short pulse of high pressure during freezing. These results were superior to our attempts using plunge freezing which did not retain the overall three-dimensional structure (results not shown). Plunge frozen embryos were flattened by the forces that occurred when the sample hit the surface of the coolant.

In the ideal case, the water is vitrified by high-pressure-freezing and no structure-damaging ice crystals are formed (Moor, 1987). The state of ice can be investigated directly by electron diffraction of frozen-hydrated cryo-sections (e.g. Michel et al., 1991). With some specimens (e.g. apple leaf) vitrification of the whole sample can be achieved (Michel et al., 1991). In many applications, however, only parts of the sample are vitrified, whereas in other zones (especially in the center of the sample) small hexagonal ice crystals form. In this study, we estimated the freezing quality by looking for ice crystal segregation patterns in the freeze-substituted TEM samples. In Fig. 3 and Fig. 4 no segregation patterns are visible. In other embryos of the same sample, small segregation patterns were visible, especially in the cell nucleus (not shown). In the presence of segregation patterns, one should be cautious with the interpretation of small structures, because they may have been altered by ice crystal formation. We do not yet know exactly, what small segregation patterns appear in the SEM and at present this limits the interpretation of the smallest structures visible in the cytoplasm at high magnification (e.g. Fig. 6).

Dehydration

In this study, some internal cell structures were made visible by cryo-fracturing. Additional structural features were then revealed by subliming some of the ice. However, considering the intimate interaction between water and biological macromolecules and the fact that many biological structures are only stable in the presence of water (e.g. membranes and in particular the half membranes that result from cryo-fracture), it is obvious that removal of water or ice always carries the risk of producing artifacts.

In this study, the ice was either removed by freeze-substitution followed by critical-point-drying or by partial freeze-drying. Freeze-substitution and critical-point-drying leads to complete dehydration of the specimen, whereas with freeze-drying it is possible to leave the specimen partially hydrated. Freeze-substitution provides chemical stabilization during dehydration, this may protect the sample from the forces occurring during critical-point-drying. However, other

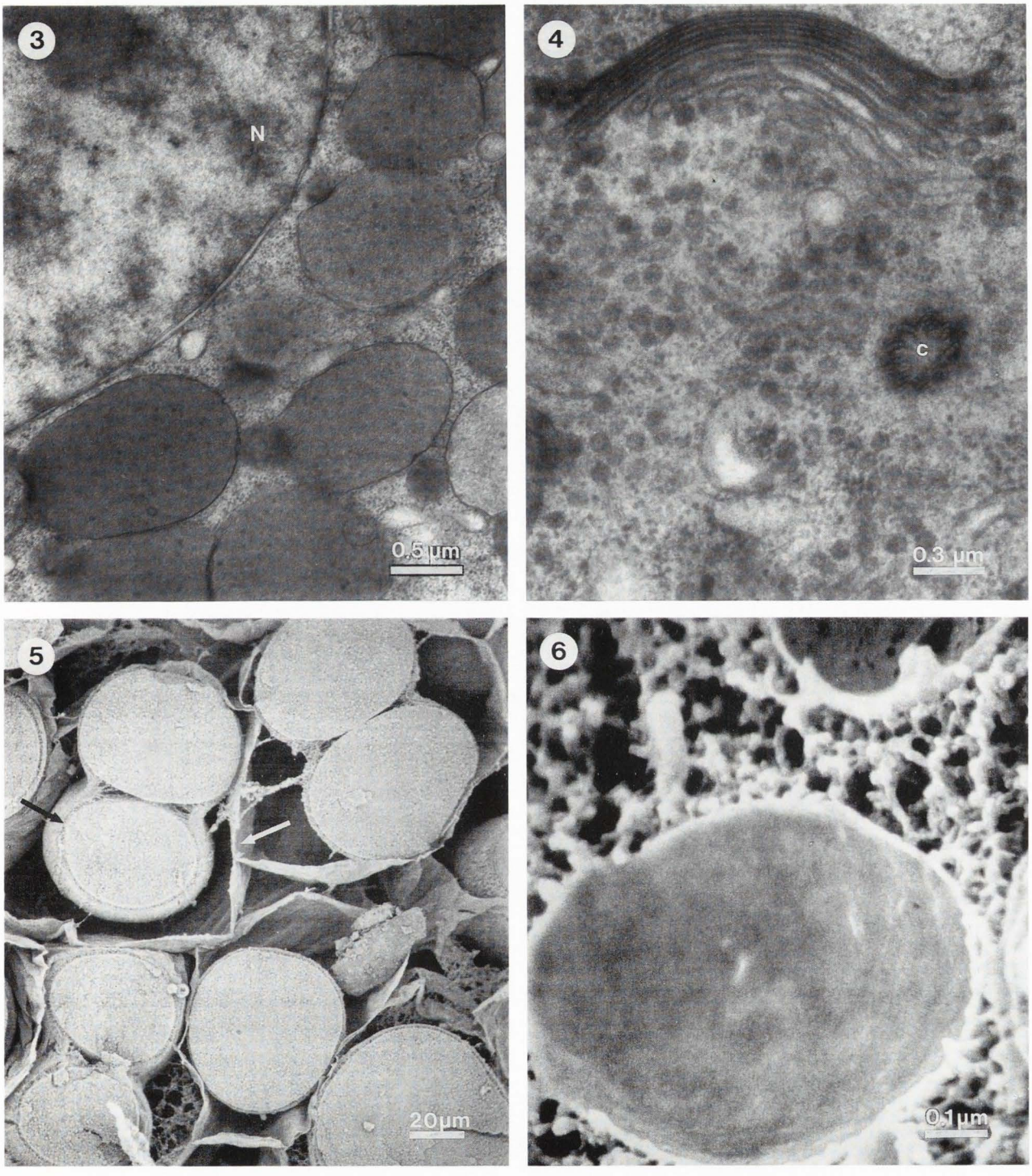

Figure 3. Portions of a high-pressure-frozen and freeze-substituted sea urchin embryo (24 h after fertilization) prepared for TEM. No major ice crystal segregation patterns are visible. The image shows the nucleus (N) with regions of chromatin at varying levels of condensation and the two membranes of the nuclear envelope. Nuclear pores can also be seen at irregular intervals. Numerous yolk granules can be seen within the cytoplasm.

Figure 4 shows the same sample at a different region in the cytoplasm. The Golgi apparatus can be seen with its numerous stacks and budding vesicles. This TEM also depicts a cross section through a centriole (C).

Figures 5 and 6. Low magnification (Figure 5) and high magnification SEM (Figure 6) of the same sample representing a 2-cell stage embryo 120 min after fertilization. The figures give an idea of the wide magnification range that can be investigated on high-pressure-frozen samples with the SEM. The black arrow on Fig. 5 depicts the hyaline layer, an extracellular matrix that is secreted after fertilization and the white arrow depicts the fertilization coat. Fig. 6 shows a high magnification of a yolk granule membrane.

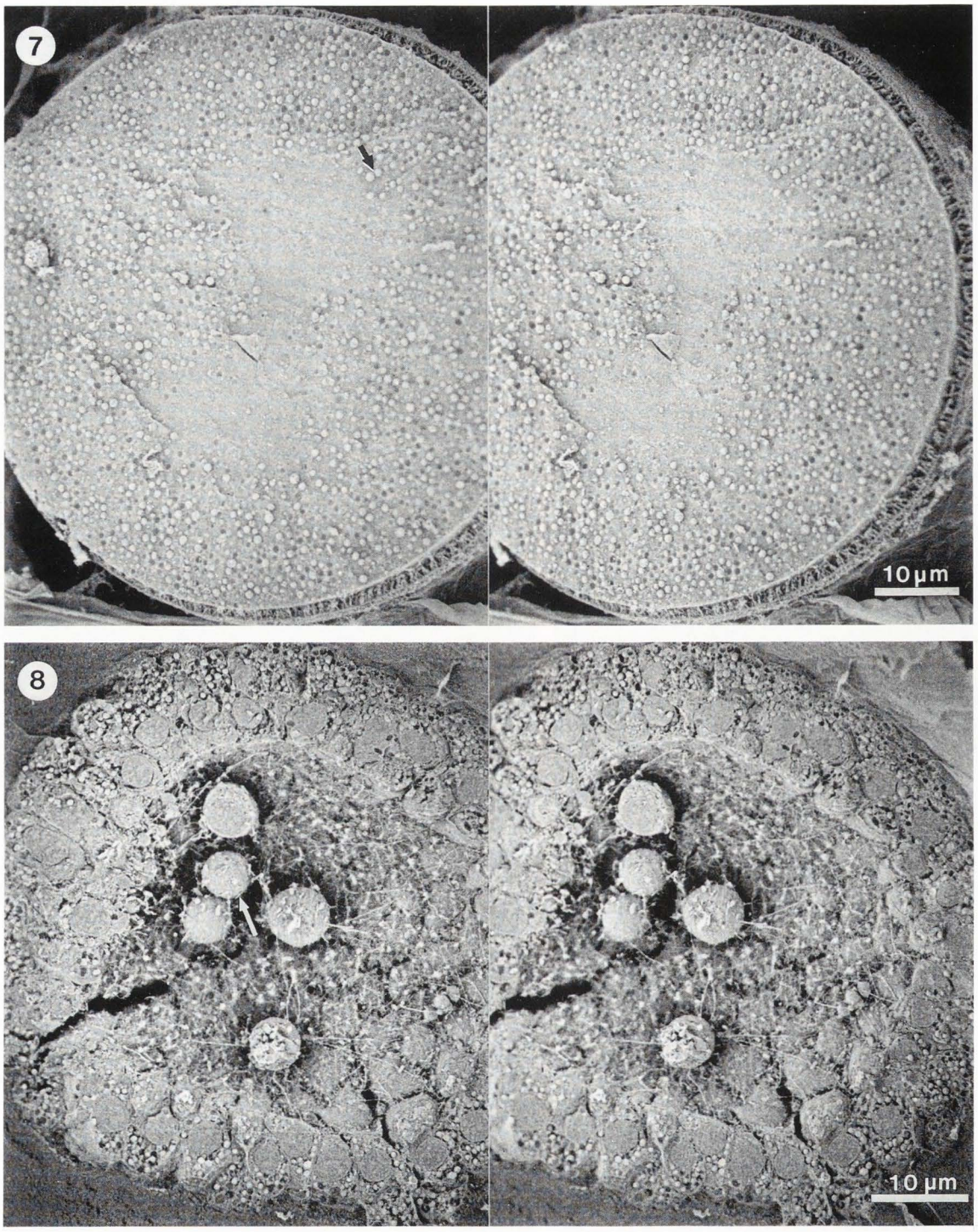

Figure 7. Stereo pair of sea urchin embryo in mitosis 1 h after fertilization. (The stereo image can be observed with a regular stereo viewer.) The clear area in the center represents the poles of the mitotic spindle and the astral microtubules. The black arrow depicts a yolk granule. The surface of this fertilized egg is covered in elongated microvilli and is surrounded by the hyaline envelope. The microvilli and the fertilization envelope are visible at the surface of the embryo.

Figure 8 shows a mesenchyme blastula stage embryo which is characterized by a layer of polarized cells surrounding a blastocoel cavity. Within the cavity can be seen the primary mesenchymal cells (arrow) which will eventually give rise to the spicules. The point at which the primary mesenchymal cell accumulate will be the point of invagination during archenteron formation.

Figures 9, 10 and 11 (opposite page) show an early gastrula stage embryo. Formation of the archenteron has begun. Fig 10 and 11 are higher magnificatons of Fig. 9. It is interesting to note the nuclear to cytoplasmic ratio as well as the heterogeneity of the nuclear contents representing either different degrees of chromatin condensation or specialized regions within the nucleus.

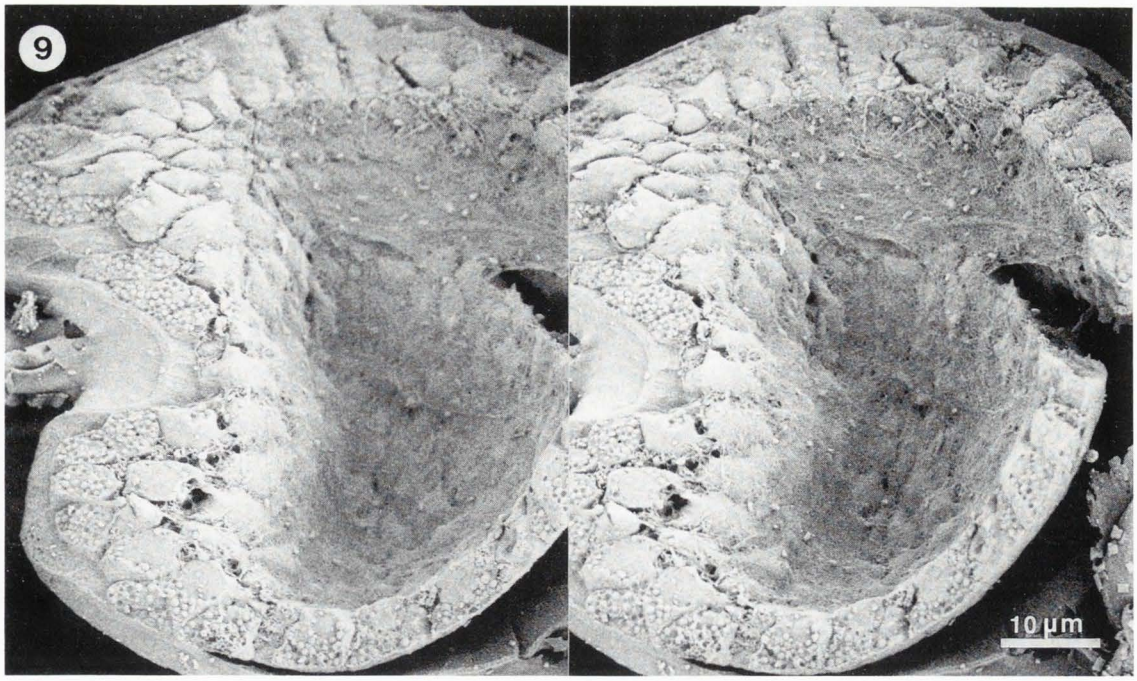
9
10 µm

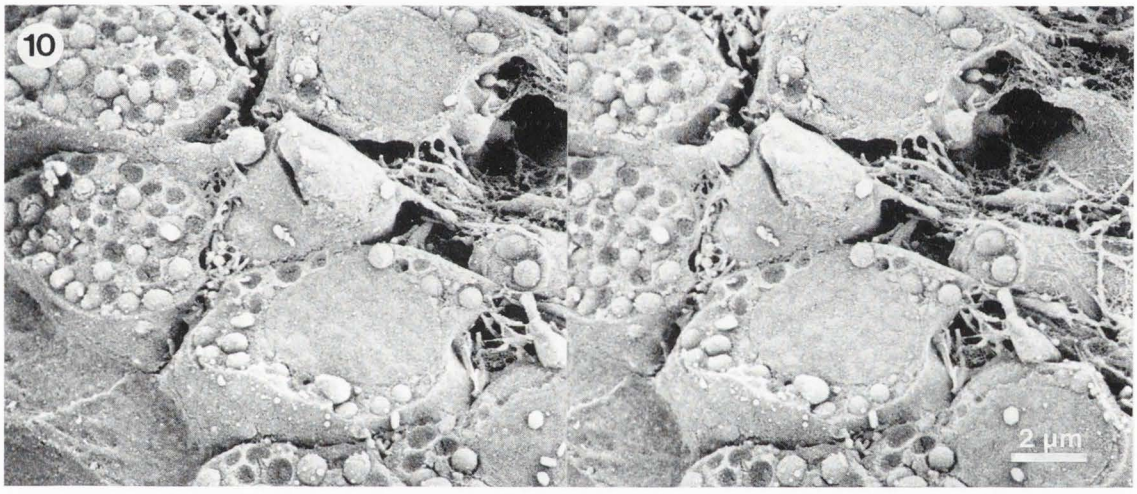
10
2 µm

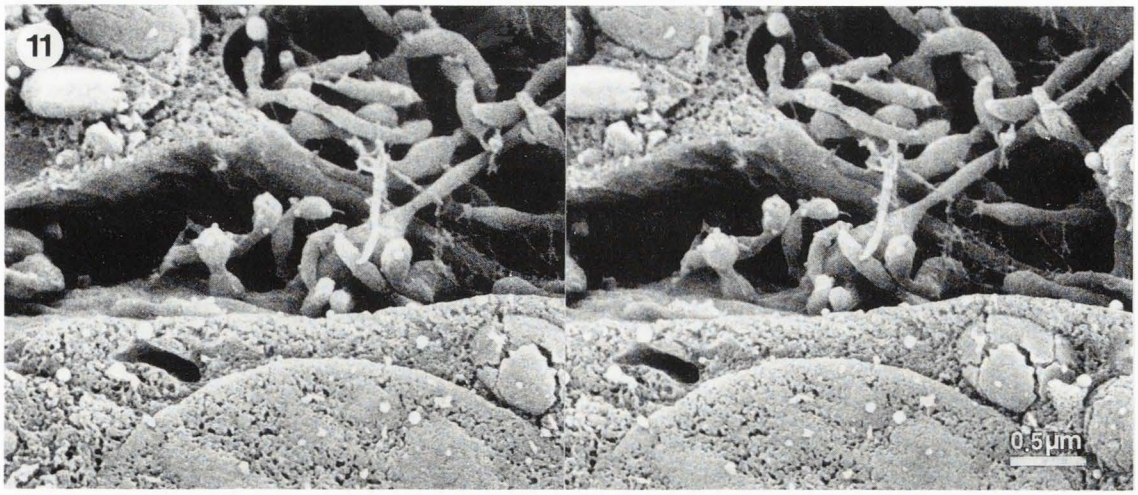
11
0.5µm

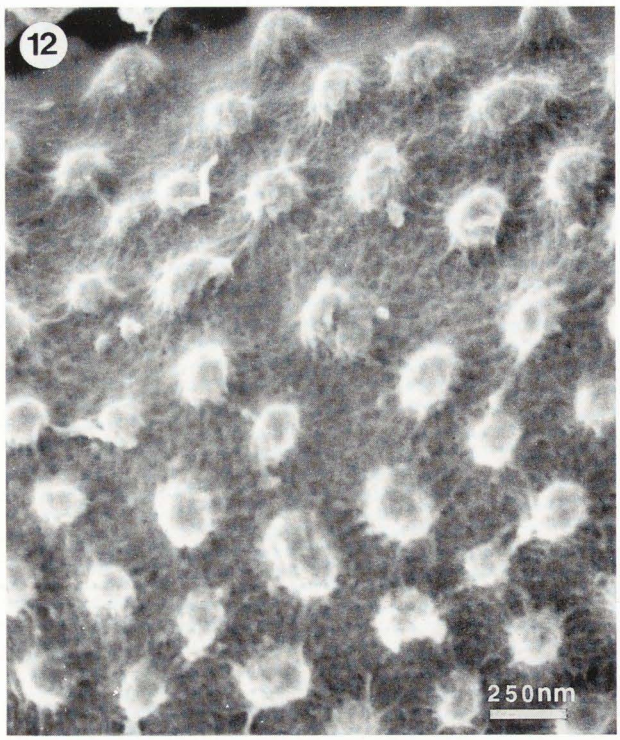

Figure 12. Surface of an unfertilized sea urchin egg, showing the short microvilli and a fine meshwork, possibly representing carbohydrate residues.

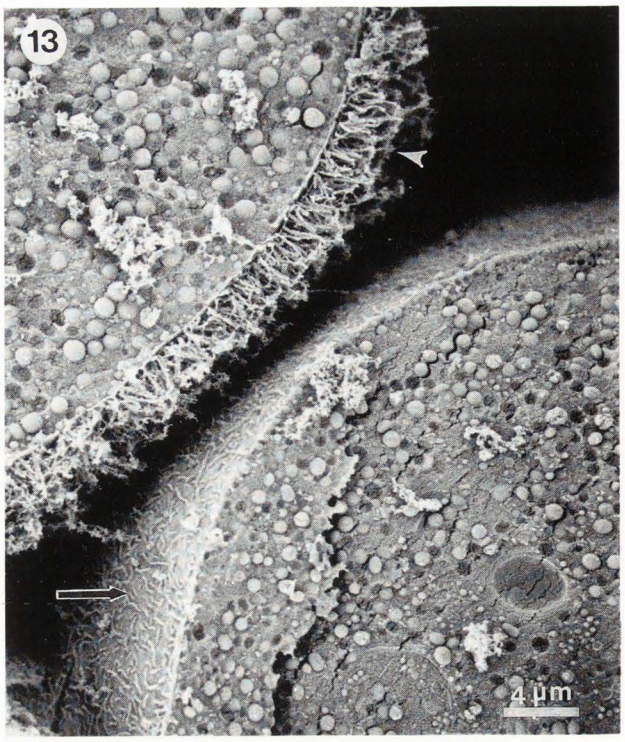

Figure 13. A freeze-fractured fertilized egg (upper left) showing long microvilli (arrowhead) and an unfertilized egg (lower right) with short microvilli (arrow).

than the work of Humbel and Müller (1986), not much basic research exists on how freeze-substitution works. Therefore, the potential and the limitations of this method in combination with critical-point-drying are not fully understood.

Freeze-drying works on purely physical principals and, therefore, may be easier to understand. When dried at 183 K, the sample showed severe drying artifacts (Fig. 15). These artifacts were reduced by partially drying the sample at about 163 K for a short time (Figs. 16 and 17). An interpretation of these results is, that after this procedure the membranes may still be mechanically stabilized by some remaining ice. By drying for 15 min at 183 K, however, too much ice is removed and the membranes collapse (Fig. 15). This interpretation implies that shrinking occurs as long as a certain amount of water is removed even when using the most careful dehydration protocol.

Coating and Microscopy

Charging artifacts represent a major problem when imaging relatively large biological objects with a high resolution SEM. Thick coating layers enhance electrical conductivity, but reduce the attainable resolution by hiding small structural details (Peters, 1986). In this work, charging was reduced by improving the contact of the embryos to the supporting gold planchets. For this purpose the embryos were frozen in a gelatine medium that provided a good connection between the dried sample and the specimen support planchet. Charging was further reduced by using the double-layer-coating technique and backscattered electron imaging (Walther and Hentschel, 1989). In addition, the samples were imaged at low voltage, which in many cases also reduces charging problems (reviewed by Pawley, 1990). The frozen-hydrated samples (Fig. 14 to 17) are less affected by charging problems. Even uncoated frozen-hydrated samples do not always show charging artefacts (Hermann and Müller, 1993; Walther et al., 1990 and 1992). On frozen-hydrated samples usually a very thin (1 to 5 nm) sputtered metal layer is applied in order to localize the secondary electron signal (Hermann and Müller, 1993).

The mass loss induced by the electron beam is a function of the hydration state of the sample. This phenomenon appears to be low on the completely dried samples (Fig. 5 to Fig. 13), allowing for the production of stereo pairs, but it is a serious limitation when observing fully hydrated samples, as shown earlier (Hermann and Müller, 1993; Walther et al., 1990 and 1992).

Acknowledgements

We thank Jon Holy for the help with operating the TEM. This work was supported by NIH Grant DDR-570 to the Integrated Microscopy Resource, Madison, WI and NIH Research Grant HD 12913 to G. P. Schatten. P. Walther was partially supported by a grant of the Swiss National Science Foundation.

References

Anderson TF. (1951). Techniques for the preservation of three-dimensional structures in preparing specimens for the electron microscope. Trans NY Acad Sci. 13: 130-133.

Autrata R, Hermann R, Müller M. (1992). An efficient single crystal BSE detector in SEM. Scanning 14, 127-135.

Barlow DI, Sleigh MA. (1979). Freeze-substitution for preservation of ciliated surfaces for scanning electron microscopy. J Microsc. 115, 81-85.

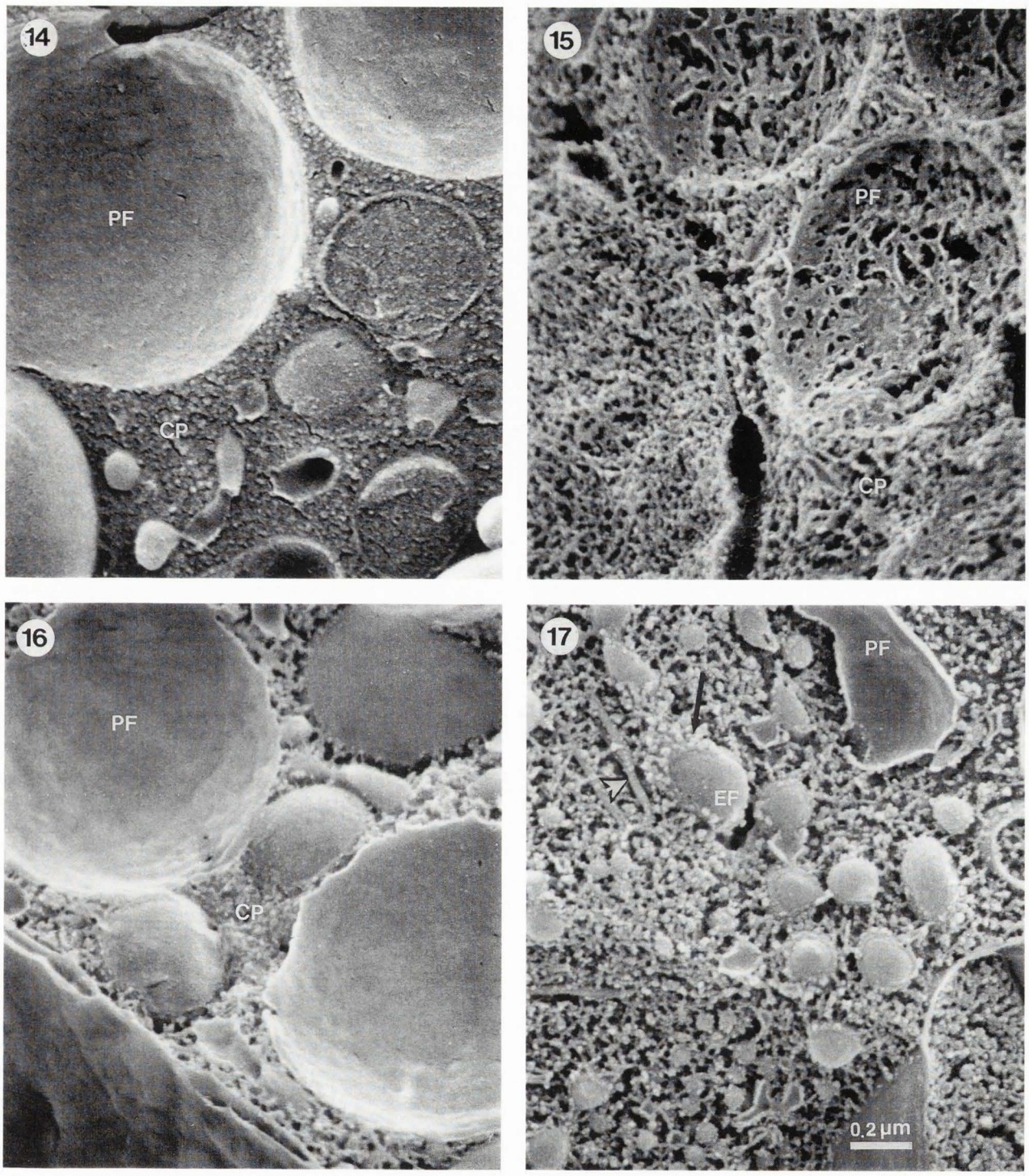

Figures 14 to 17. The effects of partial freeze-drying on a freeze-fractured portion of an embryo. Fig. 14 represents a fully hydrated sample. No shrinkage artifacts are visible. The small cracks represent damage caused by the primary beam. After drying at 183 K (Fig. 15) the membranes have collapsed because most of the supporting ice has been removed. After a shorter drying at 163 K (Figs. 16 and 17) enough ice remains bound to the lipids to prevent collapse of the crossfractured membranes (Fig. 16), however, additional structures become visible such as cytoskeletal elements (Fig. 17, arrowhead) and globular particles surrounding the small vesicles (black arrow). PF: plasmatic membrane fracture face, EF: extraplasmatic membrane fracture face, CP: cytoplasm.

Danielson P. (1987). Rough pumping without oil contamination. Res Devel. 29, 97-104.

Echlin P. (1971) The examination of biological material at low temperatures. Scanning Electron Microscopy 1971/1: 225-232.

Franks J, Clay CS, Pease GW. (1980). Ion beam thin film deposition. Scanning Electron Microsc. 1980, I: 155-162.

Hermann R, Müller M. (1991). High resolution biological scanning electron microscopy: A comparative study of low temperature metal coating techniques. J Electron Microsc Tech. 18, 440-449.

Hermann R, Müller M. (1993). Progress in Scanning Electron Microscopy of Frozen-Hydrated Biological Specimens. Scanning Microsc. 7, 343-350.

Humbel B, Müller M. (1986). Freeze-Substitution and Low Temperature Embedding. In: Müller M, Boyde A, Wolosewick JJ. (eds) Science of Biological Specimen Preparation. SEM Inc., AMF O`Hare, IL 60666-0507, USA. 175-183.

Luft JH. (1961). Improvements in epoxy resins embedding methods. J Biophys Biochem Cytol. 9, 409-414.

Michel M, Hillmann T, Müller M. (1991). Cryo-sectioning of plant material frozen at high pressure. J Microsc. 163, 3-18.

Moor H, Riehle U. (1968). Snap-freezing under high pressure: A new fixation technique for freeze-etching. In: Steve Bociarelli (ed) Electron Microscopy 1968, Vol 2. Proc 4th Eur Reg Conf Electron Microsc, Rome, pp. 33-34.

Moor H. (1987). Theory and Practice of High-pressure-Freezing. In: Cryotechniques in Biological Electron Microscopy (ed by K. Zierold & R.A. Steinbrecht) pp. 175-191. Springer-Verlag, Berlin Heidelberg.

Müller M, Marti Th, Kriz S. (1980). Improved structural preservation by freeze-substitution. Proc 7th Europ Congr on Electron Microscopy, The Hague. 2: 720-721.

Nagatani T, Saito S, Sato M, Yamada M. (1987). Development of an ultra high resloution scanning electron microscope by means of a field-emission source and in-lens system. Scanning Microsc. 1, 901-909.

Pawley JB, Erlandsen SL. (1989). The case for low voltage high resolution scanning electron microscopy of biological samples. Scanning Microsc. 3, Supplement 3, 163-178.

Pawley JB. (1990). Practical aspects of high-resolution LVSEM. Scanning. 12, 247-252.

Peters K-R. (1986). Metal deposition by high energy sputtering for high magnification electron microscopy. In: Advanced techniques in Biological Electron Microscopy. III, Koehler JK (ed), Springer Verlag Berlin. 101-166.

Reynolds EW. (1963). The use of lead citrate at high pH as an electron-opaque stain in electro microscopy. J Cell Biol. 17, 208-212.

Ris H. (1985). The cytoplasmic filament system in critical-point dried whole mounts and plastic embedded sections. J Cell Biol. 100, 1474-1487.

Sitte H, Edelmann L, Neumann K. (1987). Cryofixation without pretreatment at ambient pressure. *Cryotechniques in Biological Electron Microscopy* (ed by R.A. Steinbrecht & K. Zierold) pp. 87-113. Springer-Verlag, Berlin Heidelberg.

Studer D, Michel M, Müller M. (1989). High-pressure-freezing comes of age. Scanning Microsc. 3, Supplement 3, 253-269.

Tobler M, Freiburghaus AU. (1991) Exeptional protective power of the 4H glove defeats occupational risks in electron microscopy. J. Microsc. 163, RP1-RP2.

Walther P, Hentschel J. (1989) Improved representation of cell surface structures by freeze-substitution and backscattered electron imaging. Scanning Microsc. 3, Supplement 3, 201-211.

Walther P, Hentschel J, Herter P, Müller T, Zierold K. (1990). Imaging of intramembranous particles in frozen-hydrated cells (*Saccharomyces cerevisiae*) by high resolution cryo-SEM. Scanning 12, 300-307.

Walther P, Autrata R, Chen Y, Pawley JB. (1991). Backscattered electron imaging for high resolution surface scanning electron microscopy with a new type YAG-detector. Scanning Microsc. 5, 301-310.

Walther P, Chen Y, Peach LL, Pawley JB. (1992) High resolution electron microscopy of frozen-hydrated cells. J Microsc. 168: 169-180.

Zierold K. (1991). Cryofixation methods for ion localization in cells by electron probe microanalysis: a review. J Microsc. 161: 357-366.

Discussion with Reviewers

K. Zierold: What time resolution can be achieved by high-pressure-freezing?

Authors: "In the range of milliseconds" is the most honest answer we are able to provide at present. Studies for a more accurate answer are currently underway in several laboratories.

S. Erlandsen: Please discuss the quality of the high-pressure-freezing seen in freeze-substituted versus partially freeze-dried samples in regard to the distance from the surface of the embryo. What were the overall dimensions of the embryo and were cells lining the ceolomic cavity (in regard to the depth of the sample) preserved as well as exposed outer cells?

Authors: The relatively large planchet allowed us to freeze several layers of embryos on top of each other. The best freezing qualities are usually expected at the edge of the sample, because the fastest cooling rates are obtained there. But, freezing quality depends also on other parameters, especially on the water content of the sample. Extracellular matrix has a very high water content and, therefore, is extremely difficult to freeze without major ice crystal damage. (See also answer to next question.)

M. Solrush: Where is the extracellular matrix that is known to fill the blastocoel [compare to: Cherr GN, Summers RG, Baldwin JD, Morrill JB. (1992). Preservation and visualization of the sea urchin embryo blastocoelic extracellular matrix. J Electron Micrsoc Tech. 22. 11-22]?

Authors: The investigation of extracellular matrix by cryofixation methods is extremely difficult. Due to the very high water content, ice crystals form easily during freezing and they are usually much larger than the ice crystals within the cells. The ice crystals displace the extracellular matrix material and produce the typical ice crystal segregation patterns, a meshwork that is formed at the edges of the ice crystals. This phenomenon has been recently investigated on the extracellular matrix of cartilage by Studer et al. (1993, an abstract) and by Keene and McDonald (1993).

Cherr et al. (1992) used plunge freezing to investigate the blastocoelic extracellular matrix of sea urchin embryos. The meshwork they found (and have described as extracellular matrix structure) clearly resembles the typical ice crystal

segregation structures. This would also be in agreement with the common observation that with plunge freezing only an area up to a depth of 10 µm can be frozen without serious ice crystal damage.

At present we do not know, how well the extracellular matrix is preserved in our samples.

References: Studer D, Michel M, Wagner J, Hunziker EB. (1993). Adequately high pressure frozen extracellular cartilage matrix exhibits no meshwork structure. Europ J Cell Biol. 61, Supplement 39: 44.

Keene, D. R. & McDonald, K. (1993). The ultrastructure of the connective tissue matrix of skin and cartilage after high-pressure freezing and freeze-substitution. J. Histochem. Cytochem., 41(8):pp1141-1153.

W. P. Wergin: In Figure 15 you indicate that membranes collapse when the supporting ice is removed. Couldn't the cracks result from sublimation of the underlying ice i. e. wouldn't the expanding water vapour rupture through the coating?

Authors: The underlying water, that is leaving the sample has to pass through the fracture face during freeze drying and may well cause additional damage to this fracture face.

S. Erlandsen: Do you think the detrimental changes noted in prolonged freeze-drying of cryo-immobilized eggs corresponds to the removal of what is referred to as "bound water" and that this removal led to collapse of structure?

Authors: We would not go that far with our interpretation, because the term "bound water" has been used in a slightly fuzzy way in the electron microscopic literature. We think, that our observations base on the (trivial) fact that structures like lipid membranes are supported by the surrounding water. If enough water is removed, the membrane collapses, because without water, the lipid membrane is not stable. This simple fact has often been overseen in the literature, because shrinking studies were undertaken with either chemically fixed samples or samples fixed by adsorbing onto a carbon film.

Y. Shimada: Why was BSE-imaging used instead of the conventional secondary electron image?

Authors: We find it often helpful to add an additional (thin) carbon layer on top of the heavy metal coat. This enhances electrical conductivity (prevents charging) and enhances mechanical stability of the specimen. In order to image the underlying heavy metal coat, the material dependent BSE-signal has to be used. The secondary electron signal would image the carbon coat that is not in close contact with the biological structure (Walther and Hentschel, 1989; Walther et al., 1991; in reference list of this paper).

K. Zierold: Is the fine granularity on the surface of your cryo-fractured samples due to the metal coat or due to cellular structures, e. g. sugar residues?

Authors: The used coatings have a granularity that is finer than the smallest details visible on the pictures in this work, as shown in previous studies (Walther et al., 1991 and 1992) .

K. Zierold: Is it possible to observe the acrosome reaction of sperm and egg in high-pressure-frozen sea urchins?

Authors: This will be one of the topics of our future work.

B.A. Afzelius: It is a pity that the scanning micrographs give no new information over what is known since very long. All the features shown are those that can be seen with an interference microscope in a living egg or embryo (and are known since 100 years) or else are of doubtful relevance (the meshwork between what may or may not be a yolk granule in Fig. 6). I would be happy if the authors could convince me that at least some structure is studied at greater advantage with this method.

Authors: When introducing a relatively new methodology such as the combination of high-pressure-freezing with cryo-SEM, one can either show structures that are already known, or one can show new structures that have not been described before. If one would show new structures, the experts in the field would certainly claim these preparation artifacts due to the new method. Therefore, in this our first paper using high-pressure-freezing we found it more reasonable to reproduce features that had been already described, in order to improve the confidence into the new technology. From this point of view we are satisfied that our results are in line with the last 100 years of microscopy. It is our recent work to investigate physiological effects with high-pressure-freezing that can not be seen after conventional fixation. (Walther P, Szczesny P, Remé C E, Müller M. (1993). Light induced damage in the retina observed on samples fixed by high pressure freezing. Europ J Cell Biol. 61, Supplement 39: 45.)

It is now generally accepted that fast freezing is the method of choice for the immobilization of biological samples at a defined physiological state. High-pressure-freezing is so far the only method that allows the freezing of large areas with minimal ice crystal damage. The high resolution SEM has the unique feature not only to show details at the macromolecular level (Figs. 6, 12 and 17) but also to allow overviews over large areas (Figs. 5, 7, 8 and 9) from the same sample. These overviews can now be directly compared with the living organism in the light microscope.